Hindawi
Geofluids
Volume 2020, Article ID 8878548, 12 pages
https://doi.org/10.1155/2020/8878548

Research Article

Numerical Simulation of the Influence of Natural Fractures on Hydraulic Fracture Propagation

Song Yaobin,[1,2] Lu Weiyong ,[1,2] He Changchun,[3] and Bai Erhu[4]

[1]*Department of Mining Engineering, Luliang University, Lvliang, Shanxi 033000, China*
[2]*Key Laboratory of Maintenance and Inspection of Coal Mine Mechanical Equipment of Lvliang City, Shanxi 033000, China*
[3]*School of Civil Engineering and Architecture, East China University of Technology, Nanchang, Jiangxi 330013, China*
[4]*School of Energy Science and Engineering, Henan Polytechnic University, Jiaozuo, Henan 454000, China*

Correspondence should be addressed to Lu Weiyong; 489698551@qq.com

Received 12 June 2020; Revised 1 July 2020; Accepted 7 July 2020; Published 24 July 2020

Academic Editor: Jingmin Xu

According to the theory of plane mechanics involving the interaction of hydraulic and natural fractures, the law of hydraulic fracture propagation under the influence of natural fractures is verified using theoretical analysis and RFPA^{2D}-Flow numerical simulation approaches. The shear and tensile failure mechanisms of rock are simultaneously considered. Furthermore, the effects of the approach angle, principal stress difference, tensile strength and length of the natural fracture, and elastic modulus and Poisson's ratio of the reservoir on the propagation law of a hydraulic fracture are investigated. The following results are obtained: (1) The numerical results agree with the experimental data, indicating that the RFPA^{2D}-Flow software can be used to examine the hydraulic fracture propagation process under the action of natural fractures. (2) In the case of a low principal stress difference and low approach angle, the hydraulic fracture likely causes shear failure along the tip of the natural fracture. However, under a high stress difference and high approach angle, the hydraulic fracture spreads directly through the natural fracture along the original direction. (3) When natural fractures with a low tensile strength encounter hydraulic fractures, the hydraulic fractures likely deviate and expand along the natural fractures. However, in the case of natural fractures with a high tensile strength, the natural fracture surface is closed, and the hydraulic fracture directly passes through the natural fracture, propagating along the direction of the maximum principal stress. (4) Under the same principal stress difference, a longer natural fracture corresponds to the easier initiation and expansion of a hydraulic fracture from the tip of the natural fracture. However, when the size of the natural fracture is small, the hydraulic fracture tends to propagate directly through the natural fracture. (5) A smaller elastic modulus and larger Poisson's ratio of the reservoir result in a larger fracture initiation pressure. The presented findings can provide theoretical guidance regarding the hydraulic fracturing of reservoirs with natural fractures.

1. Introduction

In recent years, hydraulic fracturing has been widely used in the engineering practices of petroleum, natural gas, shale gas, and coal mining [1–5]. The propagation of hydraulic fractures plays a key role in the optimisation of hydraulic fracture design and represents a challenging problem corresponding to the theoretical study of hydraulic fractures [6–9]. However, in the case of fractured reservoirs, the presence of natural fractures can change the path of the hydraulic fracture propagation, leading to the formation of a complicated fracture propagation system with multibranch fractures, which increases the complexity of the hydraulic fracture network[10, 11]. Therefore, the accurate prediction and control of the hydraulic fracture morphology in fractured reservoirs is critical to improve the oil and gas production in fractured reservoirs [12–16].

Results of numerical simulation and experimental testing have indicated that the horizontal principal stress difference and approach angle corresponding to the hydraulic and natural fractures are the main factors affecting the trends of

hydraulic fractures [17–20]. Rahman et al. suggested that under a low approach angle and low stress difference, a hydraulic fracture could be easily captured, and the natural fracture could open to divert part of the fracturing fluid, thereby preventing the further expansion of the hydraulic fracture. For an intermediate approach angle, the natural fracture was open, and the passing of the hydraulic fracture through the natural fracture depended on the stress difference. Under a low stress difference, only the natural fractures opened. However, under a high stress difference, the hydraulic fractures penetrated the natural fractures. In the case of a high approach angle, the hydraulic fractures always penetrated the natural fractures, regardless of the magnitude of the stress difference. Moreover, Rahman and Rahman indicated that the change in the pore water pressure did not directly influence the interaction between hydraulic and natural fractures; this change only accelerated the resteering stress when the hydraulic fracture penetrated the natural fracture, and the pore water pressure influenced the distribution of the water stress in the natural fracture[21]. In the existing calculation model, the mechanical properties of natural fractures are not considered. Moreover, the hydraulic fractures passing through or captured by the natural fractures are identified by assuming that the friction coefficient of the natural fractures is constant. In contrast, the mechanical strength of natural fractures considerably influences the extension behaviour of hydraulic fractures [22, 23]. A mutual interference occurs between the hydraulic and natural fractures, and the natural fractures are prone to shear failure. Specifically, natural fractures inflate under the action of water pressure, resulting in a large amount of fluid loss in the natural fractures [24, 25]. Considering the impact of natural fractures on hydraulic fractures, several studies have been undertaken. However, several aspects such as whether the direction of expansion of hydraulic fractures changes under the action of natural fractures and the mechanism of change in the fracture propagation path have not been effectively addressed [26].

The equivalent plane model is one kind of the equivalent models. With the help of the equivalent plane model in this paper, the actual process is transformed and abstracted into an equivalent, simple, and easy mathematical model, which is convenient for theoretical analysis. In this study, an equivalent plane model of hydraulic and natural fractures is established by combining the stress-seepage theory with seepage-damage mechanics. Moreover, the mechanisms of shear fractures and tensile failure are considered. The RFPA^{2D}-Flow software is used to examine the mechanism of hydraulic fracture propagation under the action of natural fractures. Furthermore, the trends of the hydraulic fracture propagation under the action of the approach angle, principal stress difference, tensile strength, and length of the natural fracture are clarified. These findings not only help improve the established theory of hydraulic fracture networks but also provide theoretical support for engineering practices, such as the optimization of the arrangement of field fracturing boreholes, minimization of the interference of natural fractures in the expansion of hydraulic fractures, effective enhancement of the increase in permeability owing to the hydraulic fractures, and the development of hydraulic fractures in a fractured reservoir.

2. Plane Model and Propagation Mechanism of the Intersection of Hydraulic and Natural Fractures

2.1. Plane Model of Intersection of Hydraulic and Natural Fractures. The influence of the natural fractures on hydraulic fracture propagation depends on the position of the natural fractures. When a hydraulic fracture meets a natural fracture located near a borehole, the natural fracture gradually expands as the fluid pressure is higher than the normal stress acting on the surface of the natural fracture. The following 4 situations may occur during the continuous expansion of the hydraulic fracture: (1) When the natural fracture is in the closed state, shear failure occurs at the intersection (Figure 1(a)). Even if the path of the hydraulic fracture propagation is not affected in this case, a considerable loss of the fracturing fluid occurs. (2) The natural fracture is penetrated by the hydraulic fracture in a closed state (Figure 1(b)). (3) After the expansion of the natural fracture, the hydraulic fracture penetrates the natural fracture at their intersection point and continues to expand along the original direction (Figure 1(c)). (4) The hydraulic fracture expands from one end of the natural fracture and deviates. This phenomenon occurs because the hydraulic fracture propagates along the strike of the inflated natural fracture, and the hydraulic fracture later propagates in a direction perpendicular to the minimum principal stress (Figure 1(d)). The plane model of the intersection of hydraulic and natural fractures is shown in Figure 1.

2.2. Propagation Mechanism of the Intersection of Hydraulic and Natural Fractures. According to the relevant theories of hydraulic fracture propagation, the main hydraulic fracture of coal and rock mass expands in the direction perpendicular to the minimum horizontal principal stress after its initiation. When the hydraulic fracture propagates along the direction of the maximum horizontal principal stress, it intersects with a natural fracture. In Figure 2, the approach angle θ is the angle of intersection between the hydraulic and natural fractures. σ_1 and σ_3 denote the maximum and minimum horizontal principal stresses, respectively.

2.2.1. Hydraulic Fractures Penetrate the Natural Fractures Directly. When a hydraulic fracture intersects a natural fracture, the natural fracture does not inflate if the fluid pressure at the tip of the hydraulic fracture is less than the normal stress σ_n acting on the surface of the natural fracture. The hydraulic fracture in this case directly passes through the natural fracture and extends along the direction of the maximum horizontal principal stress. At this time, the fluid pressure in the hydraulic fracture can be expressed as follows [27, 28].

$$\tau + \sigma_t < p, \tag{1}$$

where τ is the component of the shear stress on the natural fracture under the far-field stress, σ_t is the tensile strength of the natural fracture, and p is the water pressure in the hydraulic fracture.

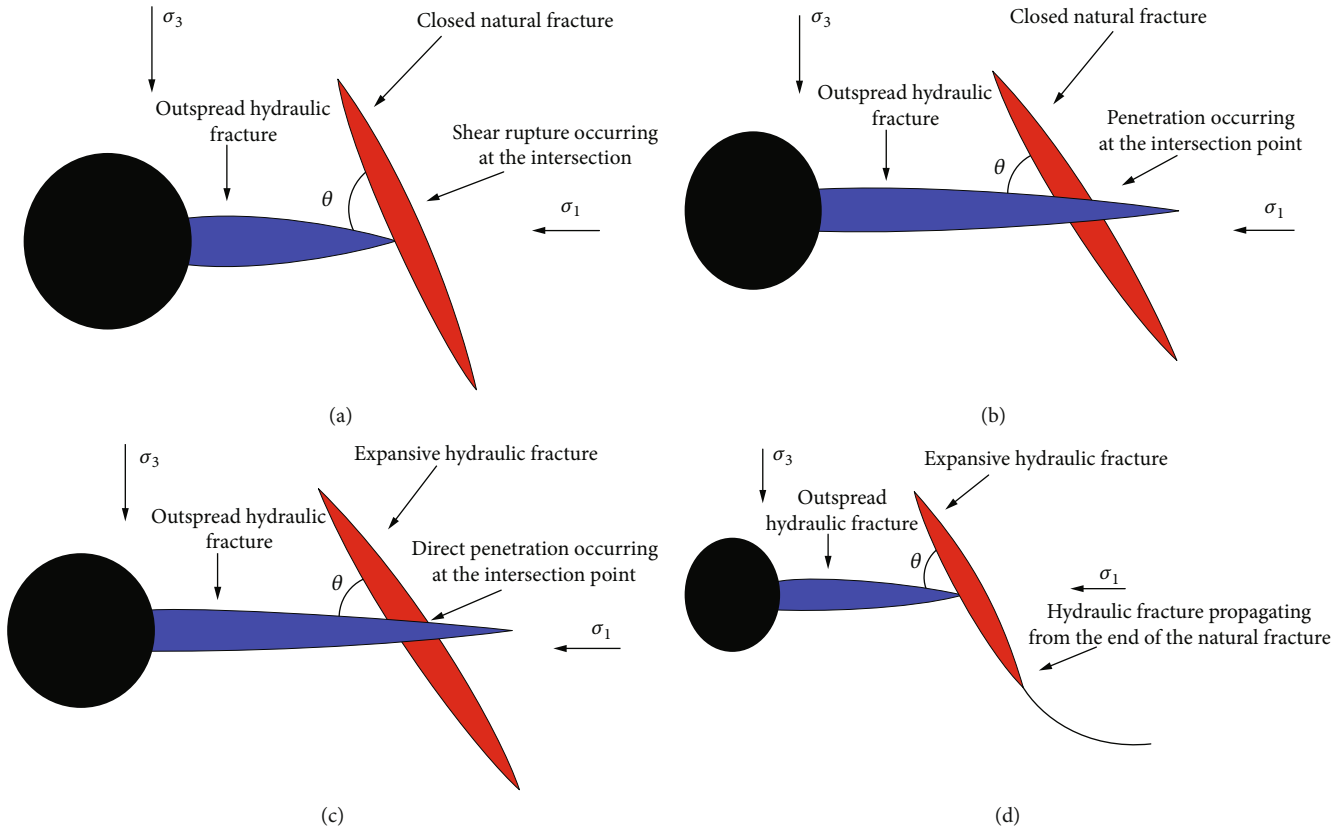

Figure 1: Plane models demonstrating the intersection of hydraulic and natural fractures. (a) Hydraulic fracture propagation when shear fracture occurs in the natural fracture. (b) Hydraulic fracture penetrates the natural fracture in the closed state directly. (c) Hydraulic fracture penetrates the natural fracture. (d) Hydraulic fracture expands from one end of the natural fracture.

According to the results of Blanton's research, the shear stress in Equation (1) can be expressed as follows [29, 30]:

$$\tau = p + (\sigma_1 - \sigma_3)(\cos 2\theta - b \sin 2\theta), \tag{2}$$

where

$$\begin{aligned} b &= \frac{1}{2a}\left[v(x_0) - \frac{x_0 - l}{K_f}\right], \\ x_0 &= \left[\frac{\left(1 + a^2\right) + e^{\pi/2K_f}}{1 + e^{\pi/2K_f}}\right]^{1/2}, \\ v(x_0) &= \frac{1}{\pi}\left[(x_0 + l)\ln\left(\frac{x_0 + l + a}{x_0 + l}\right)^2\right. \\ &\quad + (x_0 - l)\ln\left(\frac{x_0 - l - a}{x_0 - l}\right)^2 \\ &\quad \left. + a\ln\left(\frac{x_0 + l + a}{x_0 - l - a}\right)^2\right], \end{aligned} \tag{3}$$

where a is the relative sliding length of the natural fracture and l is the length of the natural fracture.

By substituting Equation (2) into Equation (1), Equation (4) can be obtained to evaluate whether the hydraulic fracture directly passes through the natural fracture.

$$\frac{\sigma_1 - \sigma_3}{\sigma_{t0}} > \frac{1}{\cos 2\theta - b \sin 2\theta}. \tag{4}$$

When Equation (4) is satisfied, the fracture directly passes through the natural fracture and propagates along the original direction. Moreover, Equation (4) indicates that the passing of the hydraulic fracture through the natural fracture is influenced by the principle stress difference $\triangle\sigma$ ($\triangle\sigma = \sigma 1\text{-}\sigma 3$), approach angle θ, tensile strength σ_t, and length l of the natural fracture, among other factors.

2.2.2. Hydraulic Fracture Propagates along the Natural Fracture. Considering the ground stress field and the orientation of the natural fractures shown in Figure 2, the normal stress σ_n and shear stress τ acting on the natural fracture surface can be obtained using a two-dimensional stress solution, which can be expressed as follows [31].

$$\sigma_n = \frac{\sigma_1 + \sigma_3}{2} + \frac{\sigma_1 - \sigma_3}{2}\cos 2(90 - \theta), \tag{5}$$

$$\tau = \frac{\sigma_1 - \sigma_3}{2} \sin 2(90 - \theta). \quad (6)$$

When the shear stress acting on the natural fracture surface is greater than the shear strength of the natural fracture surface, shear failure occurs in the natural fracture [32]. According to the linear friction theory, the mathematical condition under which this shear failure occurs is as follows [33, 34].

$$|\tau| > C_0 + K_f(\sigma_n - p), \quad (7)$$

where C_0 is the cohesion of the natural fracture and K_f is the friction coefficient of the natural fracture surface.

By substituting Equations (5) and (6) into Equation (7), the following expression can be obtained:

$$(\sigma_1 - \sigma_3)(\sin 2\theta + K_f \cos 2\theta) - K_f(\sigma_1 + \sigma_3 - 2p) > 2C_0. \quad (8)$$

The fluid pressure in the natural fracture surface must be lower than the normal stress acting on the natural fracture surface; otherwise, the fracture is opened, that is, the fluid pressure satisfies the following relation:

$$p < \frac{\sigma_1 + \sigma_3}{2} + \frac{\sigma_1 - \sigma_3}{2} \cos 2(90 - \theta). \quad (9)$$

According to the theory of fracture propagation, the Griffith linear fracture propagation requires the minimum fluid pressure. Assuming that the fracture is a Griffith fracture, the water pressure at the tip of the hydraulic fracture can be expressed as follows:

$$p = \sigma_3 + \sqrt{\frac{2E\gamma}{\pi L(1 - \mu^2)}}, \quad (10)$$

where E is the elastic modulus of the reservoir rock, γ is the surface energy per unit area of the reservoir rock, L is the half length of the Griffith fracture, and μ is the Poisson's ratio of the reservoir rock.

Hence, the following expression can be obtained:

$$\sigma_1 - \sigma_3 > \frac{2c - 2K_f\sqrt{2E\gamma/(\pi L(1 - \nu^2))}}{\sin 2\theta - K_f + K_f \cos 2\theta}. \quad (11)$$

According to Equation (11), when hydraulic fractures encounter natural fractures, the factors that determine whether the hydraulic fractures can extend along the natural fractures include the horizontal principal stress difference $\triangle\sigma$, approach angle θ, length of the natural fracture l, friction coefficient K_f, elastic modulus of the rock mass E, and Poisson's ratio μ.

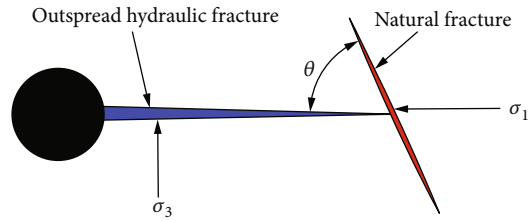

Figure 2: Plane model of a hydraulic fracture intersecting a natural fracture.

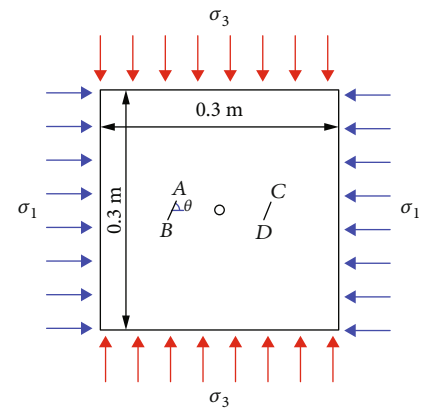

Figure 3: Geometric model.

3. Verification of Simulation Results of Hydraulic Fracture Propagation under the Influence of Natural Fractures

3.1. Geometric Model. In this paper, RFPA^{2D}-Flow software, a seepage-stress coupling analysis system for rock fracture instability, is used to analyze the interaction mechanism between natural fractures and hydraulic fractures based on the damage mechanics theory, in which both tensile and shear failure criteria of the rock are chosen[35, 36]. In this numerical simulation, a two-dimensional plane stress model (Figure 3) sized 0.5 m × 0.5 m is adopted. All the boundaries are impermeable and constrained by the confining pressure. Both the bottom and left boundaries are fixed. The centre of the borehole with a diameter of 0.02 m coincides with the centre of the model. The model is divided into 300 × 300 cells. Cracks AB and CD are arranged in advance at equal distances on the left and right sides of the borehole, respectively. The lengths and widths of the two preexisting cracks are, respectively, 0.04 m and 0.002 m. The tensile strength of the two preexisting cracks is 6.5 MPa, and the internal friction angle is 30°. The maximum principal stress σ_1 in the horizontal direction is 10 MPa, and the minimum principal stress σ_3 in the vertical direction is 5 MPa. The initial water pressure applied in the borehole is 0 MPa, and the step increment is 0.5 MPa.

3.2. Parameter Selection. To ensure that the numerical calculation can more closely simulate the real physical experiment, the actual physical parameters of the experimental sample are adopted in the numerical simulation as much as possible.

Table 1: Parameters used in the numerical simulation.

Parameter	Value and unit	Parameter	Value and unit
Tensile strength σ_t	6.5/10.5 MPa	Internal friction angle	30°
Elastic modulus E	50 GPa	Residual strength	0.1%
Compression tension ratio	10	Pore water pressure coefficient	0.1
Permeability coefficient k	0.000864 m/d	Maximum compression strain coefficient	200
Maximum tension strain coefficient	1.5	Water increment $\triangle p_w$ for each step	0.5 MPa
Initial water pressure p_{w0}	0 MPa	Vertical principle stress σ_1	5 MPa
Horizontal principle stress σ_1	10 MPa	Approach angle θ	45/90°

The relevant parameters utilized in this numerical simulation are presented in Table 1. Parameters such as compressiveness, tension strength, elastic module, and Poisson's ratio can be determined based on the experimental test. The permeability can be calculated by the laboratory experiment. Before water is poured into the fracturing borehole, there is no water pressure. Therefore, the initial water pressure is 0 MPa.

3.3. Propagation of Hydraulic Fractures under the Influence of Natural Fractures. Figure 4 indicates that (1) the hydraulic fracture penetrates the natural fracture from one end and passes through the natural fracture. Subsequently, the hydraulic fracture continues to extend along the other end of the natural fracture. In other words, the hydraulic fracture completely extends along the natural fracture, as shown in Figure 4(a). (2) When the hydraulic fracture encounters the natural fracture, it does not deviate and expand along the natural fracture but directly penetrates the natural fracture and continues to expand along the direction of the maximum horizontal stress, as shown in Figure 4(b). (3) When the hydraulic fracture encounters the natural fracture, the left hydraulic fracture deviates; after this fracture expands from one end of the natural fracture, it eventually propagates along the direction of the maximum principle stress. However, the right hydraulic fracture directly penetrates the natural fracture, as shown in Figure 4(c).

The numerical results indicate that the hydraulic fracture can propagate via three paths under the action of natural fractures. (1) The hydraulic fracture extends completely along the natural fracture. The fractures are generated around the natural fracture, and their expansion is not evident. (2) The hydraulic fracture penetrates the natural fracture and expands along the original direction. The length of the generated hydraulic fracture is considerably larger than that of the natural fracture; however, few short fractures are present around the natural fracture. (3) The hydraulic fracture propagates through and along the natural fracture simultaneously, including cases (1) and (2), resulting in a larger number of fractures and a wider distribution range. These three cases are consistent with the theoretical plane model of the intersection of the hydraulic and natural fractures. In the exploitation of oil and gas resources, the third case leads to the formation of a hydraulic fracture network and can reduce the engineering quantity, thereby improving the exploitation efficiency of the oil and gas resources.

Renshaw and Pollard et al. examined the critical approach angle of a hydraulic fracture passing through a natural fracture under different stress conditions by conducting a physical experiment and obtained the critical curve of the hydraulic fracture passing through the natural fracture (black solid line in Figure 5)[37]. The Renshaw and Pollard criterion can be used to predict the results of the interaction of the hydraulic and natural fractures. A comparison of the numerical results, indicated by the red stars and blue dots in Figure 5, and the experimental results obtained by Renshaw and Pollard et al. indicate that the numerical results are in agreement with the Renshaw and Pollard criterion. In other words, the numerical results are consistent with the experimental results.

4. Influence of Natural Fractures on the Hydraulic Fracture Propagation

The homogeneity, size, number of cells, borehole aperture, and basic mechanical parameters of the model were kept unchanged, and the single variable method was used to examine the influence of the approach angle, principle stress difference, tension strength and length of the natural fracture, elastic modulus, and Poisson's ratio on the hydraulic fracture propagation.

4.1. Influence of the Approach Angle on the Hydraulic Fracture Propagation. When the approach angle θ is 0°, 30°, 45°, 60°, and 90°, the propagation of the hydraulic fracture is as shown in Figures 6(A)–6(E), respectively. The following observations can be made: (1) When θ is 0°, 30°, and 45°, the hydraulic fracture first propagates along the direction perpendicular to the minimum principal stress σ_3. After the hydraulic fracture intersects the natural fracture, it extends along the natural fracture and propagates from one end of the natural fracture. Subsequently, the fracture deviates and continues expanding in the direction of the maximum horizontal principal stress σ_1. For a smaller angle θ, this phenomenon is more notable because a smaller θ corresponds to a smaller normal stress σ_n on the natural fracture. Consequently, a smaller shear stress τ and tensile stress σ_t are required for the sliding of the hydraulic fracture and opening of the natural fracture surface, respectively. The natural fracture opens easily, and the hydraulic fracture continues to expand along one end of the natural fracture surface. In the case of a low stress difference and approach angle, the natural

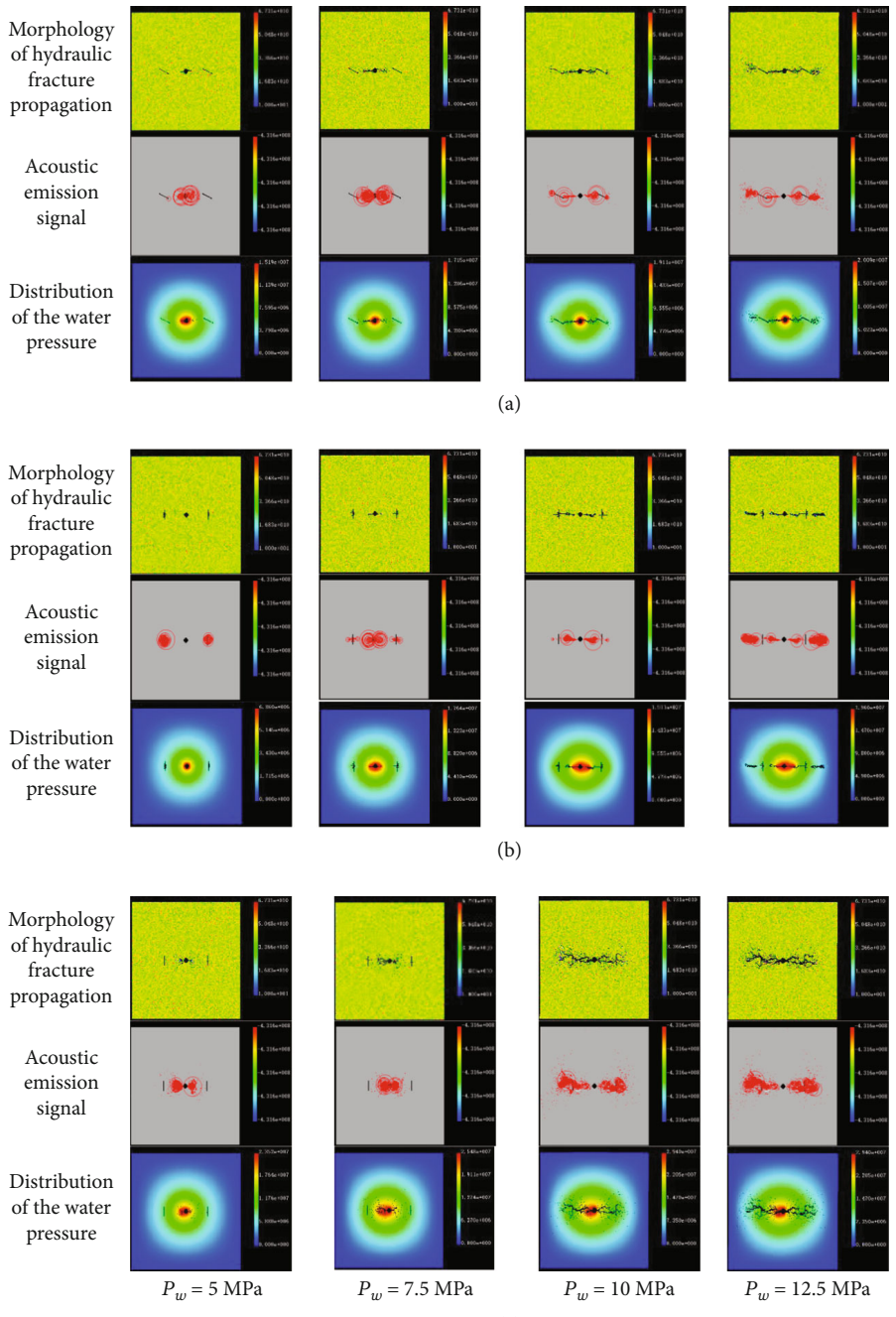

Figure 4: Propagation processes of a hydraulic fracture under the action of a natural fracture. (a) Propagation of a hydraulic fracture along a natural fracture. (b) Propagation of a hydraulic fracture penetrating the natural fracture. (c) Propagation of a hydraulic fracture through and along a natural fracture.

fracture is activated by the hydraulic fracture, and part of the pore water pressure is transferred, thus preventing the hydraulic fracture from further passing through the natural fracture. (2) When θ is 60° and 90°, the hydraulic fracture directly passes through the natural fracture, indicating that the hydraulic fracture can easily pass through the existing natural fracture under a high approach angle. This finding can be attributed to the fact that a larger approach angle θ corresponds to a larger normal stress σ_n on the natural fracture. Consequently, a greater shear stress τ tensile stress σ_t are required for the sliding of the hydraulic fracture and opening of the natural fracture surface, respectively. The natural fracture is difficult to be opened, and the hydraulic fracture penetrates the natural fracture directly.

4.2. Influence of Difference in the Main Stress on the Hydraulic Fracture Propagation. Considering the minimum main stress σ_3 as 5 MPa and the maximum main stress σ_1 as 5 MPa, 10 MPa, 15 MPa, 20 MPa, 25 MPa, and 30 MPa, the corresponding horizontal stress difference $\triangle\sigma$ is 0 MPa,

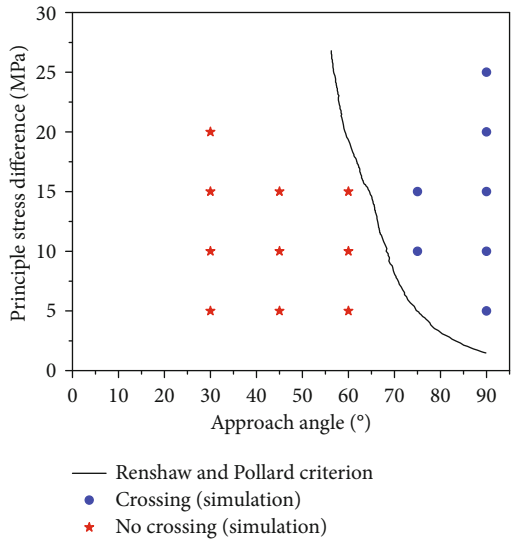

Figure 5: Comparison of numerical simulation and experimental results.

5 MPa, 10 MPa, 15 MPa, and 20 MPa, respectively. The process of hydraulic fracture propagation under different horizontal stress differences is shown in Figure 7. The following observations can be made: (1) When the horizontal stress difference $\triangle\sigma$ is 5 MPa, the hydraulic fracture first propagates along the direction perpendicular to the minimum principal stress. After intersecting with the natural fracture, the hydraulic fracture expands from one end of the natural fracture and deviates to expand along the direction of the maximum principal stress again. This finding shows that the natural fracture is activated by the hydraulic fracture, and a part of the pore water pressure is transferred under the condition of a low stress difference, thereby preventing the hydraulic fracture from further passing through the natural fracture. (2) When the horizontal stress difference $\triangle\sigma$ is 10 MPa and 15 MPa, after the hydraulic fracture intersects with the natural fracture, the hydraulic fracture on the left side propagates along the direction perpendicular to the natural fracture. Furthermore, the fluid permeates along the interface of the natural fracture. After the left hydraulic fracture permeates along the interface for a certain distance, it penetrates the interface and expands along the original direction. The hydraulic fracture on the right side penetrates directly through the natural fracture and continues expanding along the direction perpendicular to the minimum principle stress. (3) When the horizontal stress difference $\triangle\sigma$ is 20 MPa and 25 MPa, after the hydraulic fracture intersects the natural fracture, it expands along the direction of the maximum principle stress. This finding shows that the hydraulic fracture easily passes through the existing natural fracture under a high stress difference.

When the principal stress difference $\triangle\sigma$ is small, the random distribution of the crystals and defects in the rock influence the propagation process. The rupturing of the rock far from the natural fracture in the model is more notable, and the shape of the hydraulic fracture is more tortuous. At this time, the natural fracture is more likely to be opened, and the hydraulic fracture is more likely to expand along the natural fracture. With the increase in the principal stress difference $\triangle\sigma$, the propagation form of the hydraulic fracture is relatively straight and parallel to the direction of the maximum principal stress σ_1. The branch fractures at the tip of the hydraulic fracture are not significant. At this time, the hydraulic fracture is more likely to expand after penetrating the natural fracture.

4.3. Effect of Tensile Strength of the Natural Fracture on the Hydraulic Fracture Propagation. When the tension strength σ_t of the natural fracture is 6 MPa, 8 MPa, 10 MPa, 12 MPa, and 14 MPa, the process of the hydraulic fracture propagation is as shown in Figure 8. The following observations can be made: (1) When the tensile strength σ_t of the natural fracture is small, the hydraulic fracture is more likely to deviate and expand along the natural fracture. Due to the change in the stress field surrounding the natural fracture, the hydraulic fracture extends at the end of natural fracture when the hydraulic fracture approaches the natural fracture or its tip. The width of the hydraulic fracture in the extension part is considerably smaller than its initial width. (2) However, with the increase in the tensile strength, the hydraulic fracture tends to penetrate the natural fracture and expands along the direction of the maximum principal stress. This aspect can be explained by the fact that the hydraulic fractures tend to extend in the direction of the least resistance. When the tensile strength of the natural fracture surface is large, the hydraulic fracture surface does not undergo shear and tensile failure, which impedes the opening of the natural fracture in the process of hydraulic fracture propagation. However, when the tensile strength of the natural fracture is small, the weak plane characteristics of the natural fracture surface are apparent, which facilitates the propagation of the hydraulic fracture along the natural fracture. This finding shows that the propagation pattern of a hydraulic fracture is closely related to the interface material of the natural fracture. The hydraulic fracture easily expands along the direction of the least resistance instead of along the whole path. Consequently, the branch fractures occur easily.

4.4. Effect of the Natural Fracture Length on the Hydraulic Fracture Propagation. The hydraulic fracture may extend along the natural fracture. After extending for a certain distance, the branches of the hydraulic fractures tend to deviate, which is beneficial for the hydraulic fracture expansion. In some cases, the hydraulic fracture extends through the natural fracture. Under the same principal stress difference, a smaller natural fracture length l corresponds to an easier expansion of the hydraulic fracture from the natural fracture tip, as shown in Figures 9(A) and 9(B). However, in the case of a natural fracture with a larger length, the hydraulic fracture tends to directly propagate through the natural fracture, as shown in Figures 9(C)–9(E). According to Equation (11), when the principle stress difference is fixed, a smaller natural fracture can more easily satisfy the mechanical conditions of the hydraulic fracture propagating along the natural fracture. In contrast, a longer natural fracture makes it more difficult

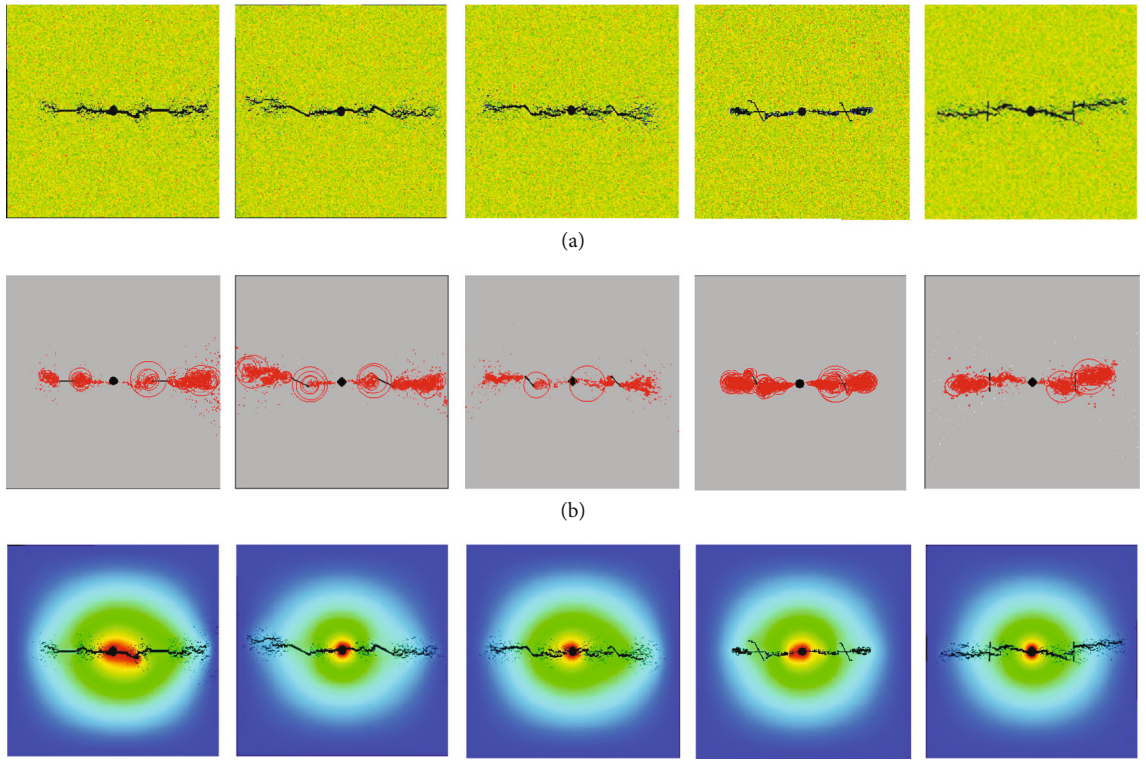

FIGURE 6: Process of hydraulic fracture propagation under different approach angles. (a) Morphology of hydraulic fracture propagation. (b) Acoustic emission signal. (c) Cloud map of pore water pressure.

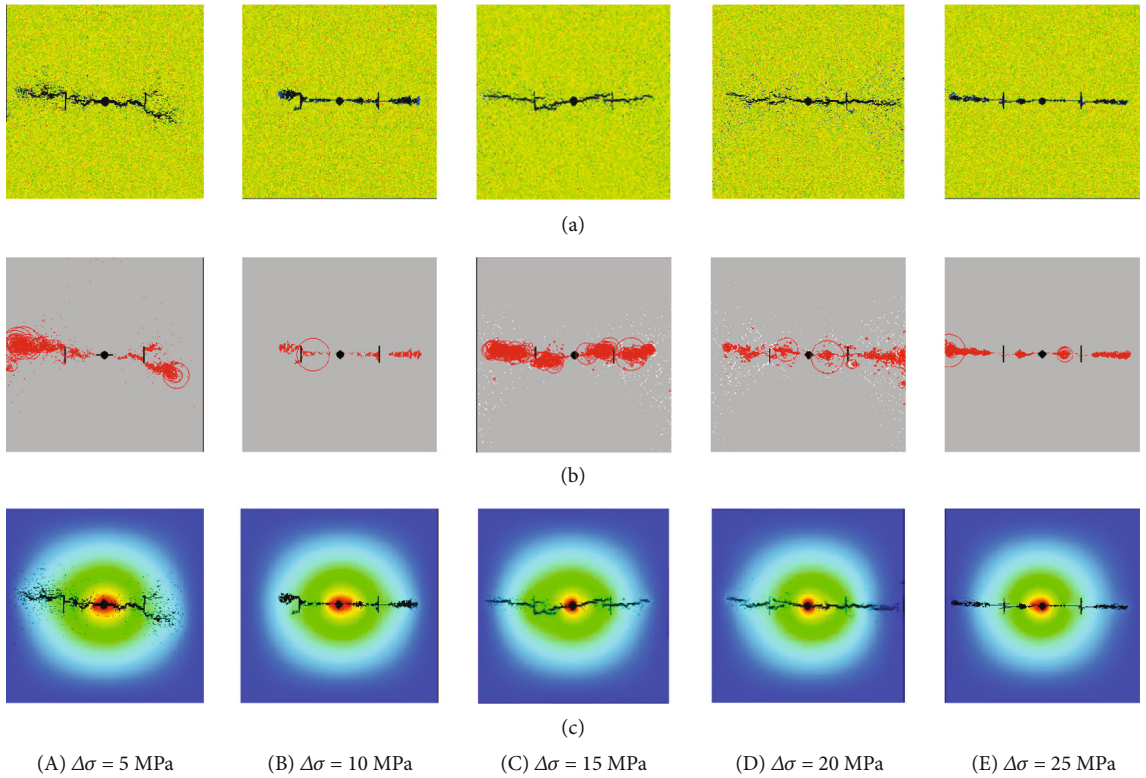

FIGURE 7: Process of hydraulic fracture propagation under different horizontal principle stress differences $\Delta\sigma$. (a) Morphology of the hydraulic fracture propagation. (b) Acoustic emission signal. (c) Cloud map of the pore water pressure.

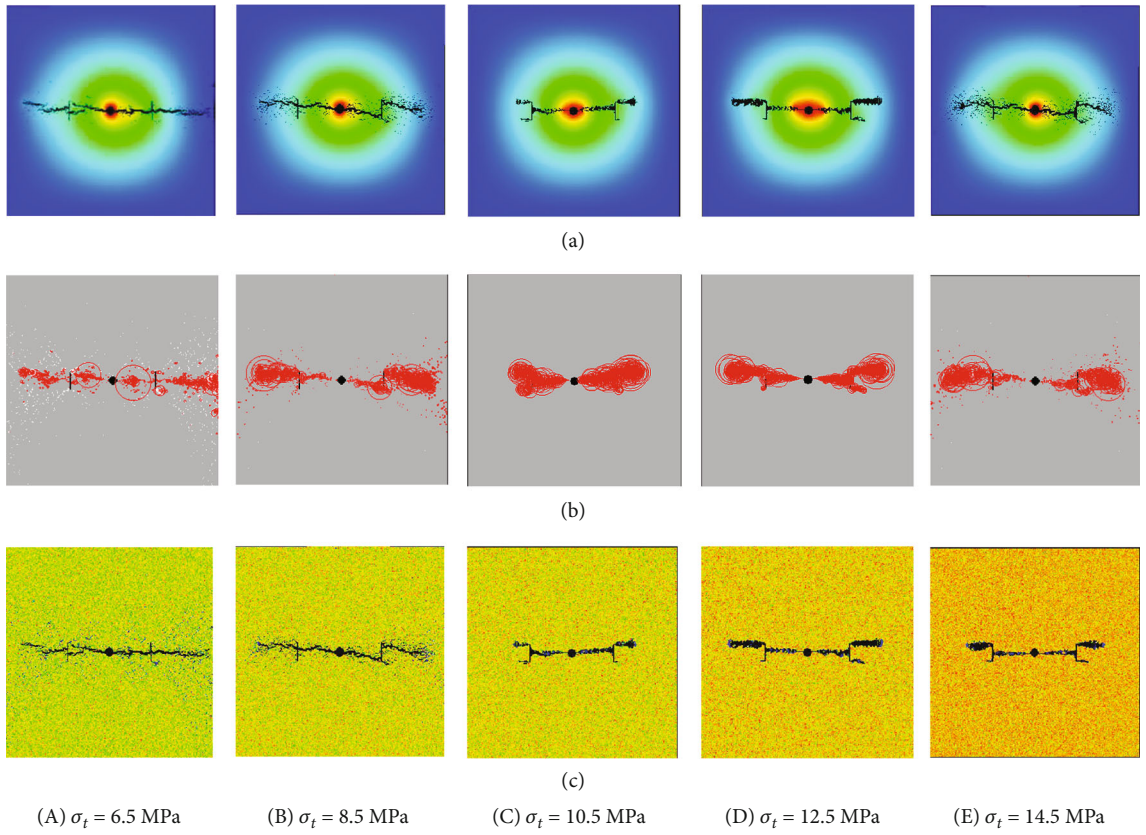

Figure 8: Process of hydraulic fracture propagation under different tensile strengths σ_t. (a) Cloud map of the pore water pressure. (b) Acoustic emission signal. (c) Morphology of the hydraulic fracture propagation.

to satisfy the mechanical conditions of the hydraulic fracture propagating along the natural fracture.

4.5. Influence of Elastic Properties of the Reservoir Rock on the Hydraulic Fracture Propagation. The elastic modulus E and Poisson's ratio μ are two important parameters to express the ability of a rock to resist deformation under the action of an external load. These two parameters are strongly related to the strength and brittleness of the rock. In general, a larger elastic modulus of the rock corresponds to a smaller Poisson's ratio. The elastic model of sedimentary rock is characterised by a higher heterogeneity. In the numerical simulation performed using the RFPA^{2D}-Flow software, both the nonuniformity of the rock strength and elastic modulus are considered. Therefore, the initiation and expansion processes of a hydraulic fracture under the action of a natural fracture, simulated using the RFPA^{2D}-Flow software, are sufficiently realistic.

The relationship between the elastic modulus of the reservoir rock and the opening pressure of the natural fracture is shown in Figure 10. The following observations can be made: (1) For a certain approach angle θ, the critical opening pressure required for a natural fracture gradually decreases with the increase in the elastic modulus E. This aspect can quantitatively explain the fact that the effect of perforation fracturing in a reservoir with a high elasticity and brittleness is more notable than that in a reservoir with a low elasticity and high toughness. (2) For a certain elastic modulus E, with the increase in the approach angle θ, the opening pressure required for the natural fracture increases. When the approach angle θ is 90°, the opening pressure of the natural fracture reaches its maximum value.

The relationship between the Poisson's ratio μ of the reservoir rock and opening pressure of the natural fracture is shown in Figure 11. The following observations can be made: (1) For a certain approach angle θ, when the Poisson's ratio μ is small, the opening pressure of the natural fracture is also small. With the increase in the Poisson's ratio μ, the opening pressure of the natural fracture increases. In particular, a reservoir with a higher elastic modulus usually has a smaller Poisson's ratio. Therefore, the influence of the elastic modulus and Poisson's ratio on the opening pressure of the natural fracture is consistent. (2) For a certain Poisson's ratio, with the increase in the approach angle, the opening pressure of the natural fracture also increases. When the approach angle θ is 90°, the opening pressure of the natural fracture exhibits its maximum value.

5. Discussion

The influence of natural fractures on hydraulic fracture propagation has been always a hot topic. In this paper, only two natural fractures are chosen. In fact, the number of the natural fractures is far more than two natural fractures in

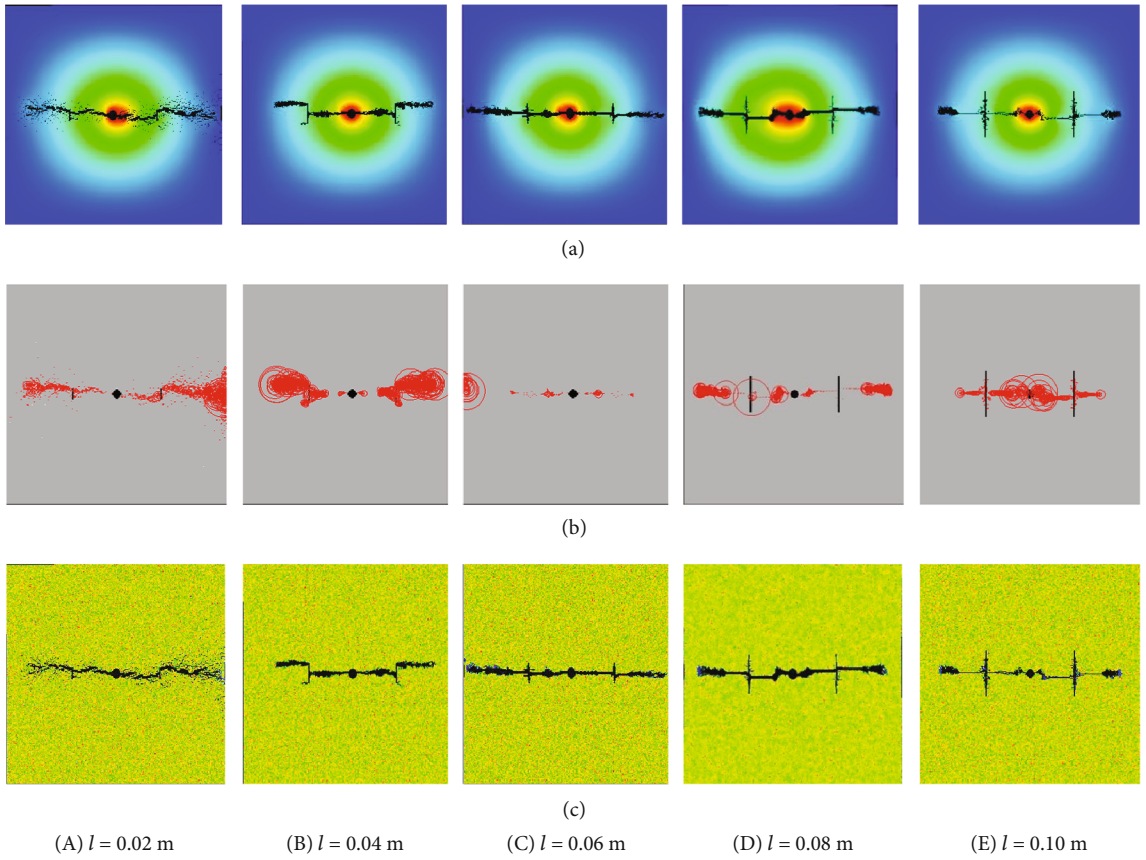

Figure 9: Process of hydraulic fracture propagation under different natural fracture lengths l. (a) Cloud map of the pore water pressure. (b) Acoustic emission signal. (c) Morphology of the hydraulic fracture propagation.

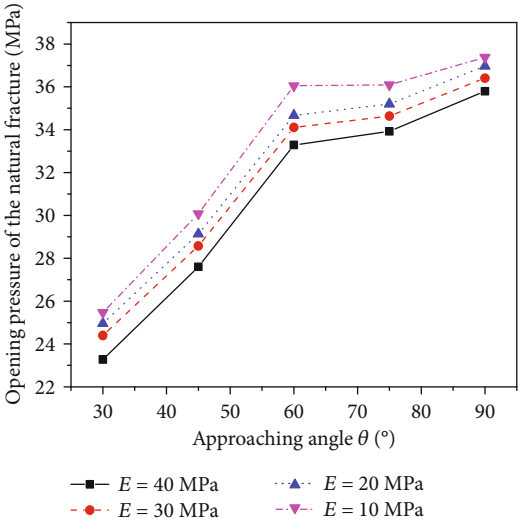

Figure 10: Opening pressure of the natural fracture under different elastic moduli.

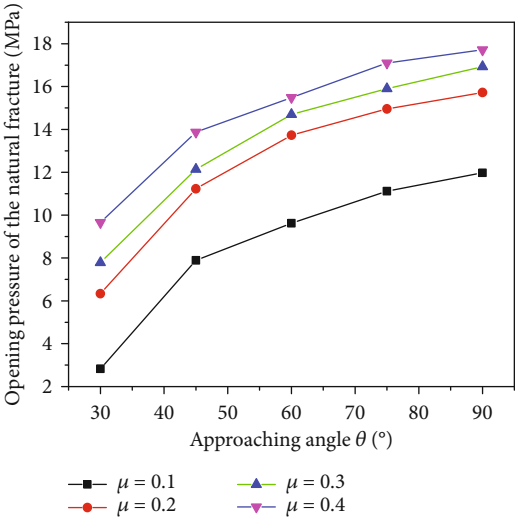

Figure 11: Opening pressure of the natural fracture under different Poisson's ratios.

the fractured reservoir. In the next research, more natural fractures should be adopted in the numerical model. Of course, the plane model and propagation mechanism of the intersection of hydraulic and natural fractures will become more complex.

RFPA^{2D}-Flow is a good numerical computational software, which can realize the visualization of the hydraulic fracture process. However, the process of the numerical simulation depends on the increment step, not the time. Therefore, much more dependent variable, such as water

pressure, length, and width of the hydraulic fracture and the like, which regard time as independent variable, cannot be obtained.

6. Conclusions

(1) Considering the tensile and shear failure mechanisms of rock rupture, a theoretical model for the hydraulic fracture propagation under the action of a natural fracture is established based on the equivalent plane fracture theory of hydraulic and natural fractures. The morphology of the hydraulic fracture determined using the numerical simulation is in agreement with the existing physical experiment results.

(2) In the case of a large approach angle, the hydraulic fracture directly passes through the natural fracture, and the initiation pressure of the natural fracture gradually increases. When the approach angle is 90°, the initiation pressure of the natural fracture reaches its maximum value. When the approach angle is small, the hydraulic fracture expands along the natural fracture, propagates from one end, and deviates and continues expanding along the direction of the maximum horizontal principal stress.

(3) Under a low principle stress difference, the hydraulic fracture tends to expand along the natural fracture, and the development of the hydraulic fracture is relatively complex. However, with the increase in the principal stress difference, the hydraulic fracture tends to penetrate the natural fracture. This aspect shows that under a low principal stress difference, the natural fracture is more likely to be opened, which facilitates the development of the hydraulic fracture.

(4) When the tensile strength of the natural fracture is large, the hydraulic fracture cannot induce shear and tensile failure, which impedes the opening of the natural fracture and the propagation of the hydraulic fracture. In contrast, when the tensile strength of the natural fracture is small, the weak surface features of the natural fracture are prominent, which facilitates the opening of the natural fracture.

(5) With the increase in the elastic modulus or decrease in the Poisson's ratio, the critical opening pressure of the natural fracture decreases. Since the reservoir rock with a higher elastic modulus usually has a smaller Poisson's ratio, the influence of the elastic modulus and Poisson's ratio on the opening pressure of the natural fracture is consistent.

Data Availability

The data in the manuscript can be available on request through Weiyong Lu, whose email address is 489698551@qq.com.

Conflicts of Interest

The authors declare that they have no known competing financial interests or personal relationships that could have appeared to influence the work reported in this paper.

Acknowledgments

The authors would like to particularly thank Dalian Mechsoft Co. Ltd for their help in providing the free RFPA^{2D}-Flow software for three months. This work was supported by the Transformation of Scientific and Technological Achievements Programs (TSTAP) of Higher Education Institutions in Shanxi (No. 2020CG050), the Special Project of 2019 Plan for the Introduction of High-Level Scientific and Technological Talents in Development Zone of Lvliang City (development of automatic disassembly platform for hydraulic support pin shaft) (No. 2019L0002), the Science and Technology Project of Lvliang City in 2019 (pressure relief and permeability improvement technology by integrated hydraulic flushing and cutting for low permeability coal seam containing methane) (No. 2019L0008), and the National Natural Science Foundation of China (Nos. 51774111 and 51974105).

References

[1] W. Lu, B. Huang, and X. Zhao, "A review of recent research and development of the effect of hydraulic fracturing on gas adsorption and desorption in coal seams," *Adsorption Science & Technology*, vol. 37, no. 5-6, pp. 509–529, 2019.

[2] S. Tripoppoom, J. Xie, R. Yong et al., "Investigation of different production performances in shale gas wells using assisted history matching: hydraulic fractures and reservoir characterization from production data," *Fuel*, vol. 267, article 117097, 2020.

[3] G. Gunarathna and B. G. Da Silva, "Influence of the effective vertical stresses on hydraulic fracture initiation pressures in shale and engineered geothermal systems explorations," *Rock Mechanics and Rock Engineering*, vol. 52, no. 11, pp. 4835–4853, 2019.

[4] L. Zhai, H. Zhang, D. Pan et al., "Optimisation of hydraulic fracturing parameters based on cohesive zone method in oil shale reservoir with random distribution of weak planes," *Journal of Natural Gas Science and Engineering*, vol. 75, article 103130, 2020.

[5] L. Cheng, D. Wang, R. Cao, and R. Xia, "The influence of hydraulic fractures on oil recovery by water flooding processes in tight oil reservoirs: an experimental and numerical approach," *Journal of Petroleum Science and Engineering*, vol. 185, article 106572, 2020.

[6] P. Behnoudfar, M. B. Asadi, A. Gholilou, and S. Zendehboudi, "A new model to conduct hydraulic fracture design in coalbed methane reservoirs by incorporating stress variations," *Journal of Petroleum Science and Engineering*, vol. 174, pp. 1208–1222, 2019.

[7] K. Cao, P. Siddhamshetty, Y. Ahn, R. Mukherjee, and J. S. I. Kwon, "Economic model-based controller design framework for hydraulic fracturing to optimize shale gas production and water usage," *Industrial & Engineering Chemistry Research*, vol. 58, no. 27, pp. 12097–12115, 2019.

[8] J. Wang, Z. Wang, B. Sun, Y. Gao, X. Wang, and W. Fu, "Optimization design of hydraulic parameters for supercritical CO_2 fracturing in unconventional gas reservoir," *Fuel*, vol. 235, pp. 795–809, 2019.

[9] X. Wang, X. Peng, S. Zhang, Y. Liu, F. Peng, and F. Zeng, "Guidelines for economic design of multistage hydraulic fracturing, Yanchang tight formation, Ordos Basin," *Natural Resources Research*, vol. 29, no. 2, pp. 1413–1426, 2020.

[10] C. R. Tiedeman and W. Barrash, "Hydraulic tomography: 3D hydraulic conductivity, fracture network, and connectivity in mudstone," *Groundwater*, vol. 58, no. 2, pp. 238–257, 2019.

[11] X. Zhao, Z. Rui, X. Liao, and R. Zhang, "The qualitative and quantitative fracture evaluation methodology in shale gas reservoir," *Journal of Natural Gas Science & Engineering*, vol. 27, no. P2, pp. 486–495, 2015.

[12] T. Guo, Z. Rui, Z. Qu, and N. Qi, "Experimental study of directional propagation of hydraulic fracture guided by multi-radial slim holes," *Journal of Petroleum Science and Engineering*, vol. 166, no. 3, pp. 592–601, 2018.

[13] Z. Rui, T. Guo, Q. Feng, Z. Qu, N. Qi, and F. Gong, "Influence of gravel on the propagation pattern of hydraulic fracture in the glutenite reservoir," *Journal of Petroleum Science & Engineering*, vol. 165, no. 7, pp. 627–639, 2018.

[14] Y. He, S. Cheng, Z. Sun, Z. Chai, and Z. Rui, "Improving oil recovery through fracture injection and production of multiple fractured horizontal wells," *Journal of Energy Resources Technology*, vol. 142, no. 5, pp. 1–19, 2020.

[15] S. Liu, L. Zhang, K. Zhang, J. Zhou, H. He, and Z. Hou, "A simplified and efficient method for water flooding production index calculations in low permeable fractured reservoir," *Journal of Energy Resources Technology*, vol. 141, no. 11, article 112905, 2019.

[16] L. Zhu, Y. Shengchao, Z. Weibing et al., "Dynamic loading induced by the instability of voussoir beam structure during mining below the slope," *International Journal of Rock Mechanics and Mining Sciences*, vol. 132, no. 6, article 104343, 2020.

[17] H. Zheng, C. Pu, and C. T. Il, "Study on the interaction mechanism of hydraulic fracture and natural fracture in shale formation," *Energies*, vol. 12, no. 23, p. 4477, 2019.

[18] H. Fatahi, M. M. Hossain, and M. Sarmadivaleh, "Numerical and experimental investigation of the interaction of natural and propagated hydraulic fracture," *Journal of Natural Gas Science and Engineering*, vol. 37, pp. 409–424, 2017.

[19] W. Xu, Y. Li, J. Zhao, X. Chen, and S. S. Rahman, "Simulation of a hydraulic fracture interacting with a cemented natural fracture using displacement discontinuity method and finite volume method," *Rock Mechanics and Rock Engineering*, vol. 53, no. 7, pp. 3373–3382, 2020.

[20] W. Xu, J. Zhao, S. S. Rahman, Y. Li, and Y. Yuan, "A comprehensive model of a hydraulic fracture interacting with a natural fracture: analytical and numerical solution," *Rock Mechanics and Rock Engineering*, vol. 52, no. 4, pp. 1095–1113, 2019.

[21] M. M. Rahman and S. S. Rahman, "Studies of hydraulic fracture-propagation behavior in presence of natural fractures: fully coupled fractured-reservoir modeling in poroelastic environments," *International Journal of Geomechanics*, vol. 13, no. 6, pp. 809–826, 2013.

[22] W. Yao, S. Mostafa, Z. Yang, and G. Xu, "Role of natural fractures characteristics on the performance of hydraulic fracturing for deep energy extraction using discrete fracture network (DFN)," *Engineering Fracture Mechanics*, vol. 230, article 106962, 2020.

[23] S. Han, Y. Cheng, Q. Gao, C. Yan, Z. Han, and X. Shi, "Analysis of instability mechanisms of natural fractures during the approach of a hydraulic fracture," *Journal of Petroleum Science and Engineering*, vol. 185, article 106631, 2020.

[24] B. Shen, T. Siren, and M. Rinne, "Modelling fracture propagation in anisotropic rock mass," *Rock Mechanics & Rock Engineering*, vol. 48, no. 3, pp. 1067–1081, 2015.

[25] P. L. Clarke and R. Abedi, "Modeling the connectivity and intersection of hydraulically loaded cracks with in situ fractures in rock," *International Journal for Numerical & Analytical Methods in Geomechanics*, vol. 42, no. 14, pp. 1592–1623, 2018.

[26] O. Kolawole and I. Ispas, "Interaction between hydraulic fractures and natural fractures: current status and prospective directions," *Journal of Petroleum Exploration and Production Technology*, vol. 10, no. 4, pp. 1613–1634, 2020.

[27] C. Song, Y. Lu, B. Xia, and H. Ke, "Effects of natural fractures on hydraulic fractures propagation of coal seams," *Journal of Northeastern University (Natural Science)*, vol. 35, no. 5, pp. 756–760, 2014.

[28] X. Liu, Y. Ding, P. Luo, and L. Liang, "Influence of natural fracture on hydraulic fracture propagation," *Special Oil and Gas Reservoirs*, vol. 2, no. 25, pp. 148–153, 2018.

[29] T. L. Blanton, "Propagation of hydraulically and dynamically induced fractures in naturally fractured reservoirs," *Society of Petroleum Engineers*, vol. 5, no. 15261, pp. 1–15, 1986.

[30] T. L. Blanton, "An experimental study of interaction between hydraulically induced and pre-existing fractures," *Society of Petroleum Engineers*, vol. 8, no. 10847, pp. 559–562, 1982.

[31] Y. Lu, C. Song, Y. Jia et al., "Analysis and numerical simulation of hydrofracture crack propagation in coal-rock bed," *Cmes-computer Modeling in Engineering & Sciences*, vol. 105, no. 1, pp. 69–86, 2015.

[32] C. Song, Y. Lu, H. Tang, and Y. Jia, "A method for hydrofracture propagation control based on non-uniform pore pressure field," *Journal of Natural Gas Science and Engineering*, vol. 33, pp. 287–295, 2016.

[33] W. Song, J. Zhao, and Y. Li, "Hydraulic fracturing simulation of complex fractures growth in naturally fractured shale gas reservoir," *Arabian Journal for Science and Engineering*, vol. 39, no. 10, pp. 7411–7419, 2014.

[34] W. Cheng, Y. Jin, M. Chen, T. Xu, Y. Zhang, and C. Diao, "A criterion for identifying hydraulic fractures crossing natural fractures in 3D space," *Petroleum Exploration and Development Online*, vol. 41, no. 3, pp. 371–376, 2014.

[35] W. Lu, Y. Wang, and X. Zhang, "Numerical simulation on the basic rules of multihole linear codirectional hydraulic fracturing," *Geofluids*, vol. 2020, Article ID 6497368, 14 pages, 2020.

[36] W. Lu and C. He, "Numerical simulation of the fracture propagation of linear collaborative directional hydraulic fracturing controlled by pre-slotted guide and fracturing boreholes," *Engineering Fracture Mechanics*, vol. 235, article 107128, 2020.

[37] C. E. Renshaw and D. D. Pollard, "An experimentally verified criterion for propagation across unbounded frictional interfaces in brittle, linear elastic materials," *International Journal of Rock Mechanics and Mining Sciences & Geomechanics Abstracts*, vol. 32, no. 3, pp. 237–249, 1995.